

---

# Toward Certified Robustness Against Real-World Distribution Shifts

---

**Haoze Wu\***  
Stanford University  
haozewu@stanford.edu

**Teruhiro Tagomori\***  
Stanford University/NRI Secure  
teruhiro@stanford.edu

**Alexandar Robey\***  
University of Pennsylvania  
arobey1@seas.upenn.edu

**Fengjun Yang\***  
University of Pennsylvania  
fengjun@seas.upenn.edu

**Nikolai Matni**  
University of Pennsylvania  
fnmatni@seas.upenn.edu

**George Pappas**  
University of Pennsylvania  
pappasg@seas.upenn.edu

**Hamed Hassani**  
University of Pennsylvania  
hassani@seas.upenn.edu

**Corina Păsăreanu**  
Carnegie Mellon University/NASA Ames  
pcorina@andrew.cmu.edu

**Clark Barrett**  
Stanford University  
barrett@cs.stanford.edu

## Abstract

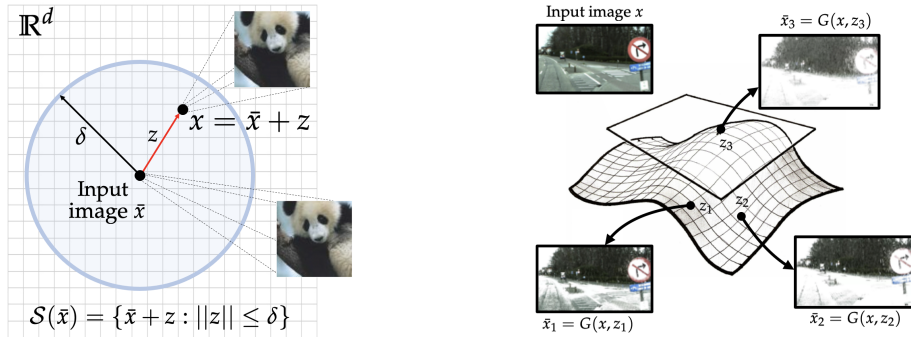
We consider the problem of certifying the robustness of deep neural networks against real-world distribution shifts. To do so, we bridge the gap between hand-crafted specifications and realistic deployment settings by proposing a novel neural-symbolic verification framework, in which we train a generative model to learn perturbations from data and define specifications with respect to the output of the learned model. A unique challenge arising from this setting is that existing verifiers cannot tightly approximate sigmoid activations, which are fundamental to many state-of-the-art generative models. To address this challenge, we propose a general meta-algorithm for handling sigmoid activations which leverages classical notions of counter-example-guided abstraction refinement. The key idea is to “lazily” refine the abstraction of sigmoid functions to exclude spurious counter-examples found in the previous abstraction, thus guaranteeing progress in the verification process while keeping the state-space small. Experiments on the MNIST and CIFAR-10 datasets show that our framework significantly outperforms existing methods on a range of challenging distribution shifts.

## 1 Introduction

Despite remarkable performance in various domains, it is well-known that deep neural networks (DNNs) are susceptible to seemingly innocuous variation in their input data. Indeed, recent studies have conclusively shown that DNNs are vulnerable to a diverse array of changes ranging from norm-bounded perturbations [1–7] to distribution shifts in weather conditions in perception tasks [8–12]. To address these concerns, there has been growing interest in using formal methods to obtain rigorous verification guarantees for neural networks with respect to particular specifications [13–50]. A key component of verification is devising specifications that accurately characterize the expected

---

\*Equal contributions.



(a) **Norm-bounded perturbation sets.** The majority of the verification literature has focused on a limited set of specifications, such as  $\ell_p$ -norm bounded perturbations, wherein perturbations can be defined by simple analytical expressions.

(b) **Real-world perturbation sets.** Most real-world perturbations cannot be described by simple analytical expressions. For example, obtaining a simple expression for a perturbation set  $\mathcal{S}(x)$  that describes variation in snow would be very challenging.

**Figure 1: Perturbation sets.** We illustrate two examples of perturbation sets  $\mathcal{S}(x)$ .

behavior of a DNN in *realistic deployment settings*. Designing such specifications is crucial for ensuring that the corresponding formal guarantees are meaningful and practically relevant.

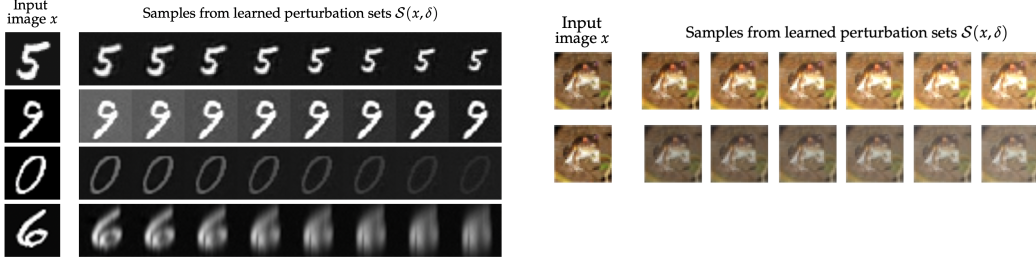
By and large, the DNN verification community has focused on specifications described by simple analytical expressions. This line of work has resulted in a set of tools which cover specifications such as certifying the robustness of DNNs against norm-bounded perturbations [14, 31, 44, 51]. However, the practical implications of these specifications are unclear beyond the realm of malicious security threats [52], as distribution shifts often cannot be described via a set of simple equations. While progress has been made toward broadening the range of specifications [53–56], it remains a crucial open challenge to narrow the gap between formal specifications and distribution shifts.

Outside of the verification community, a simultaneous line of work has shown that deep generative models can be trained to provably capture real-world distribution shifts [8, 9, 57, 58]. In particular, this body of work has shown that latent variables in generative adversarial networks [8, 57] and variational autoencoders [9] can capture relevant shifts in applications such as graph contrastive learning [59], medical imaging [58, 60], and autonomous perception [8, 9]. And while this progress has resulted in several robust training algorithms, the few verification schemes that leverage these tools assume that the generative models are piecewise-linear functions [56, 61], thereby excluding state-of-the-art architectures which heavily rely on transcendental activations (e.g., sigmoid) [62].

To bridge the gap between formal verification tools and application-driven deployment settings, in this paper we introduce a new framework for verifying the robustness of DNNs against real-world distribution shifts. Distribution shifts often cannot be described by simple analytical expressions; in the absence of such expressions, our key insight is to use deep generative models—trained to provably capture distribution shifts—to define specifications in a neural-symbolic verification framework [63]. To support state-of-the-art generative models in this framework, we propose a novel abstraction-refinement algorithm for handling transcendental activation functions. We show that this innovation significantly boosts verification precision when compared to existing approaches.

**Contributions.** Our contributions are as follows:

- We introduce a new framework for verifying DNNs against real-world distribution shifts.
- We are the first to incorporate deep generative models that capture distribution shifts—e.g. changes in weather conditions or lighting in perception tasks—into verification specifications.
- We propose a novel abstraction-refinement strategy for transcendental activation functions.
- We show that our verification techniques are significantly more precise than existing techniques on a range of challenging real-world distribution shifts on MNIST and CIFAR-10.



(a) **MNIST samples.** From top to bottom, the distribution shifts are scale, brightness, contrast, and Gaussian blur.

(b) **CIFAR-10 samples.** The distribution shifts for these sets are brightness (top) and fog (bottom).

**Figure 2: Samples from learned perturbation sets.** We show samples from two learned perturbation sets  $\mathcal{S}(x, \delta)$  on the MNIST and CIFAR-10 datasets. Samples were generated by gridding the latent space of  $\mathcal{S}(x, \delta)$ .

## 2 Problem formulation

In this section, we formally define the problem of verifying the robustness of DNN-based classifiers against real-world distribution shifts. The key step in our problem formulation is to propose a unification of logical specifications with deep generative models which capture distribution shifts.

**Neural network classification.** We consider classification tasks where the data consists of instances  $x \in \mathbb{X} \subseteq \mathbb{R}^{d_0}$  and corresponding labels  $y \in [k] := \{1, \dots, k\}$ . The goal of this task is to obtain a classifier  $C_f : \mathbb{R}^d \rightarrow [k]$  such that  $C_f$  can correctly predict the label  $y$  of each instance  $x$  for each  $(x, y)$  pair. In this work, we consider classifiers  $C_f(x)$  defined by  $C_f(x) = \arg \max_{j \in [k]} f_j(x)$ , where we take  $f : \mathbb{R}^{n_0} \rightarrow \mathbb{Y} \subseteq \mathbb{R}^{d_L}$  (with  $d_L = k$ ) to be an  $L$ -layer feed-forward neural network with weights and biases  $\mathbf{W}^{(i)} \in \mathbb{R}^{d_i \times d_{i-1}}$  and  $\mathbf{b}^{(i)} \in \mathbb{R}^{d_i}$  for each  $i \in \{1, \dots, L\}$  respectively. More specifically, we let  $f(x) = \mathbf{n}^{(L)}(x)$  and recursively define

$$\mathbf{n}^{(i)}(x) = \mathbf{W}^{(i)} \left( \hat{\mathbf{n}}^{(i-1)}(x) \right) + \mathbf{b}^{(i)}, \quad \hat{\mathbf{n}}^{(i)}(x) = \rho \left( \mathbf{n}^{(i)}(x) \right), \quad \text{and} \quad \hat{\mathbf{n}}^{(0)}(x) = x. \quad (1)$$

Here,  $\rho$  is a given activation function (e.g., ReLU, sigmoid, etc.) and  $\mathbf{n}^{(i)}$  and  $\hat{\mathbf{n}}^{(i)}$  represent the pre- and post-activation values of the  $i^{\text{th}}$  layer of  $f$  respectively.

**Perturbation sets and logical specifications.** The goal of DNN verification is to determine whether or not a given *logical specification* regarding the behavior of a DNN holds in the classification setting described above. Throughout this work, we use the symbol  $\Phi$  to denote such logical specifications, which define relations between the input and output of a DNN, i.e.,  $\Phi := (\Phi_{\text{in}}(x) \Rightarrow \Phi_{\text{out}}(y))$ . For example, given a fixed instance-label pair  $(\bar{x}, \bar{y})$ , the specification

$$\Phi := (\|\bar{x} - x\|_p \leq \epsilon \implies C_f(x) = \bar{y}) \quad (2)$$

captures the property of robustness against norm-bounded perturbations by checking whether all points in an  $\ell_p$ -norm ball centered at  $\bar{x}$  are classified by  $C_f$  as having the label  $\bar{y}$ .

Although the study of specifications such as (2) has resulted in numerous verification tools, there are many problems which cannot be described by this simple analytical model, including settings where data varies due to distribution shifts. For this reason, it is of fundamental interest to generalize such specifications to capture more general forms of variation in data. To do so, we consider abstract *perturbation sets*  $\mathcal{S}(x)$ , which following [9] are defined as “a set of instances that are considered to be equivalent to [a fixed instance]  $x$ .” An example of an abstract perturbation set is illustrated in Figure 1b, wherein each instance in  $\mathcal{S}(x)$  shows the same street sign with varying levels of snow. Ultimately, as in the case of norm-bounded robustness, the literature surrounding abstract perturbation sets has sought to train classifiers to predict the same output for each instance in  $\mathcal{S}(x)$  [8, 9, 57].

**Learning perturbation sets from data.** Designing abstract perturbation sets  $\mathcal{S}(x)$  which accurately capture realistic deployment settings is critical for providing meaningful guarantees. Recent advances in the generative modeling community have shown that distribution shifts can be *provably* captured by deep generative models. The key idea in this line of work is to parameterize perturbation sets  $\mathcal{S}(x)$  in the latent space  $\mathcal{Z}$  of a generative model  $G(x, z)$ , where  $G$  takes as input an instance  $x$

and a latent variable  $z \in \mathcal{Z}$ . Prominent among such works is [9], wherein the authors study the ability of conditional variational autoencoders (CVAEs) to capture shifts such as variation in lighting and weather conditions in images. In this work, given a CVAE parameterized by  $G(x, \mu(x) + z\sigma(x))$ , where  $\mu(x)$  and  $\sigma(x)$  are neural networks, the authors consider abstract perturbation sets of the form

$$\mathcal{S}(x) := \{G(x, \mu(x) + z\sigma(x)) : \|z\| \leq \delta\}. \quad (3)$$

Under favorable optimization conditions, the authors of [9] prove that CVAEs satisfy two statistical properties which guarantee that the data belonging to learned perturbation sets in the form of (3) produce realistic approximations of the true distribution shift (c.f. Assumption 1 and Thms. 1 and 2 in [9]). To further verify this theoretical evidence, we show that this framework successfully captures real-world shifts on MNIST and CIFAR-10 in Figure 2.

**Verifying robustness against learned distribution shifts.** To bridge the gap between formal verification methods and perturbation sets which accurately capture real-world distribution shifts, our approach in this paper is to incorporate perturbation sets parameterized by deep generative models into verification routines. We summarize this setting in the following problem statement.

**Problem 2.1.** Given a DNN-based classifier  $C_f(x)$ , a fixed instance-label pair  $(\bar{x}, \bar{y})$ , and an abstract perturbation set  $\mathcal{S}(\bar{x})$  in the form of (3) that captures a real-world distribution shift, our goal is to determine whether the following neural-symbolic specification holds:

$$\Phi := (x \in \mathcal{S}(\bar{x}) \implies C_f(x) = \bar{y}) \quad (4)$$

In other words, our goal is to devise methods which verify whether a given classifier  $C_f$  outputs the correct label  $y$  for each instance in a perturbation set  $\mathcal{S}(x)$  parameterized by a generative model  $G$ .

### 3 Technical approach and challenges

The high-level idea of our approach is to consider the following equivalent specification to (4), wherein we absorb the generative model  $G$  into the classifier  $C$ :

$$\Phi := (\|z\| \leq \delta \implies C_{Q_z}(\bar{x}) = \bar{y}) \quad (5)$$

Here,  $Q_z(x) = (f \circ G)(x, \mu(x) + z\sigma(x))$  is the concatenation of the deep generative model  $G$  with the DNN  $f$ . While this approach has clear parallels with verification schemes within the norm-bounded robustness literature, there is a *fundamental technical challenge*: state-of-the-art generative models heavily rely on sigmoid activations to produce realistic data; however, the vast majority of the literature concerning DNN verification considers DNNs that are piece-wise linear functions. For completeness, below we provide a general definition of sigmoid activations.

**Definition 3.1** (Inflection point). A function  $f : \mathbb{R} \rightarrow \mathbb{R}$  has an inflection point at  $\eta$  iff it is twice differentiable at  $\eta$ ,  $f''(\eta) = 0$ , and  $f'$  changes sign as its argument increases through  $\eta$ .

**Definition 3.2** (Sigmoid). A sigmoid function  $\rho : \mathbb{R} \rightarrow \mathbb{R}$  is a bounded, twice differentiable function which has a non-negative derivative at each point and has exactly one inflection point.

**Verification with sigmoid activations.** There are a few verification techniques that can handle sigmoid functions [18, 31, 34, 51, 64, 65]. They rely on abstraction, which builds an over-approximation of the network behavior, but suffer from imprecision, especially when verifying a neural network on large input domains. Fig. 3 shows an abstraction of the popular logistic activation function  $\sigma(x) = \frac{1}{1+e^{-x}}$ . If the specification holds on the abstracted network (where the sigmoid activation is abstracted with the convex region), then it holds on the original network. However, if a counter-example to the specification is found when using the abstraction, it may be spurious (as shown in the figure), and the specification might still hold on the precise, un-abstracted network.

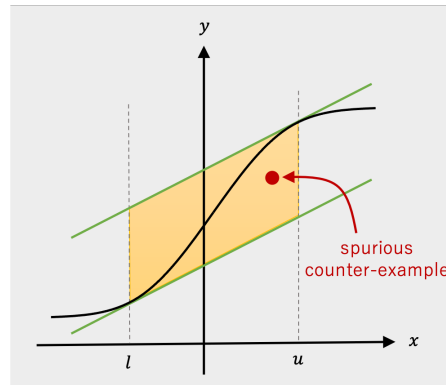


**Figure 3:** An abstraction of the sigmoid activation function.

---

**Algorithm 1** VNN-CEGAR( $M := \langle \mathcal{V}, \mathcal{X}, \mathcal{Y}, \phi_{\text{aff}}, \phi_{\rho} \rangle, \Phi$ )

---

```
1: function VNN-CEGAR( $M := \langle \mathcal{V}, \mathcal{X}, \mathcal{Y}, \phi_{\text{aff}}, \phi_{\rho} \rangle, \Phi$ )
2:    $M' \leftarrow \text{Abstract}(M)$ 
3:   while true do
4:      $\langle \alpha, \text{proven} \rangle \leftarrow \text{Prove}(M', \Phi)$  ▷ Try to prove.
5:     if proven then return true ▷ Property proved.
6:      $\langle M', \text{refined} \rangle \leftarrow \text{Refine}(M', \Phi, \alpha)$  ▷ Try to refine.
7:     if  $\neg \text{refined}$  then return false ▷ Counter-example is real.
```

---

This spurious behavior of existing verifiers demonstrates that there is a need for *refinement* of abstraction-based methods to improve the precision. For piecewise-linear activations, there is a natural refinement step: case splitting on the activation phases. However, in the case of sigmoid activations, it is less clear how to perform this refinement, because if the refinement is performed too aggressively, the state space may explode and exceed the capacity of current verifiers. To address this technical challenge, we propose a counter-example guided refinement strategy for sigmoid activation functions which is based on the CEGAR approach [66]. Our main idea is to limit the scope of the refinement to the region around a specific counter-example. In the next section, we formally describe our proposed framework and we show that it can be extended to other transcendental activation functions (e.g., softmax).

## 4 A CEGAR framework for sigmoid activations

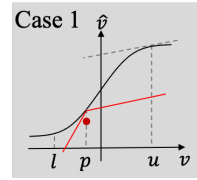
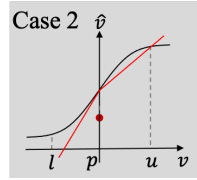
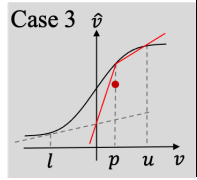
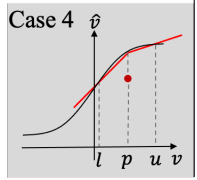
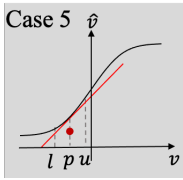
In this section, we formalize our meta-algorithm for precisely reasoning about DNNs with sigmoid activations, which is based on the CEGAR framework [67]. We first present the general framework and then discuss concrete instantiations of the sub-procedures.

**Verification preliminaries.** Our procedure operates on tuples of the form  $M := \langle \mathcal{V}, \mathcal{X}, \mathcal{Y}, \phi_{\text{aff}}, \phi_{\rho} \rangle$ . Here,  $\mathcal{V}$  is a set of real variables with  $\mathcal{X}, \mathcal{Y} \subseteq \mathcal{V}$  and  $\phi_{\text{aff}}$  and  $\phi_{\rho}$  are sets of formulas over  $\mathcal{V}$  (when the context is clear, we also use  $\phi_{\text{aff}}$  and  $\phi_{\rho}$  to mean the conjunctions of the formulas in those sets). A *variable assignment*  $\alpha : \mathcal{V} \mapsto \mathbb{R}$  maps variables in  $\mathcal{V}$  to real values. We consider properties of the form  $\Phi := (\Phi_{\text{in}}(\mathcal{X}) \Rightarrow \Phi_{\text{out}}(\mathcal{Y}))$ , where  $\Phi_{\text{in}}(\mathcal{X})$  and  $\Phi_{\text{out}}(\mathcal{Y})$  are linear arithmetic formulas over  $\mathcal{X}$  and  $\mathcal{Y}$ , and we say that  $\Phi$  holds on  $M$  if and only if the formula  $\psi := \phi_{\text{aff}} \wedge \phi_{\rho} \wedge \Phi_{\text{in}}(\mathcal{X}) \wedge \neg \Phi_{\text{out}}(\mathcal{Y})$  is unsatisfiable. We use  $M \models \Phi$  to denote that  $\Phi$  holds ( $\psi$  is unsatisfiable),  $M[\alpha] \models \neg \Phi$  to denote that  $\Phi$  does not hold and is falsified by  $\alpha$  ( $\psi$  can be satisfied with assignment  $\alpha$ ), and  $M[\alpha] \models \Phi$  to denote that  $\Phi$  is not falsified by  $\alpha$  ( $\alpha$  does not satisfy  $\psi$ ). Given this notation, we define a sound abstraction as follows:

**Definition 4.1** (Sound abstraction). *Given a tuple  $M := \langle \mathcal{V}, \mathcal{X}, \mathcal{Y}, \phi_{\text{aff}}, \phi_{\rho} \rangle$  and a property  $\Phi = (\Phi_{\text{in}}(X) \Rightarrow \Phi_{\text{out}}(Y))$ , we say the tuple  $M' := \langle \mathcal{V}' \supseteq \mathcal{V}, \mathcal{X}, \mathcal{Y}, \phi'_{\text{aff}}, \phi'_{\rho} \rangle$  is a sound abstraction of  $M$  if  $M' \models \Phi$  implies that  $M \models \Phi$ .*

**Verifying DNNs.** Given a DNN  $f$ , we construct a tuple  $M_f$  as follows: for each layer  $i$  in  $f$ , we let  $\mathbf{v}^{(i)}$  be a vector of  $d_i$  variables representing the pre-activation values in layer  $i$ , and let  $\hat{\mathbf{v}}^{(i)}$  be a similar vector representing the post-activation values in layer  $i$ . Let  $\hat{\mathbf{v}}^{(0)}$  be a vector of  $n_0$  variables from  $\mathcal{V}$  representing the inputs. Then, let  $\mathcal{V}$  be the union of all these variables, and let  $\mathcal{X}$  and  $\mathcal{Y}$  be the input and output variables, respectively; that is,  $\mathcal{X}$  consists of the variables in  $\hat{\mathbf{v}}^{(0)}$ , and  $\mathcal{Y}$  contains the variables in  $\mathbf{v}^{(L)}$ .  $\phi_{\text{aff}}$  and  $\phi_{\rho}$  capture the affine and non-linear (i.e., activation) transformations in the neural network, respectively. In particular, for each layer  $i$ ,  $\phi_{\text{aff}}$  contains the formulas  $\mathbf{v}^{(i)} = \mathbf{W}^{(i)} \hat{\mathbf{v}}^{(i-1)} + \mathbf{b}^{(i)}$ , and  $\phi_{\rho}$  contains the formulas  $\hat{\mathbf{v}}^{(i)} = \rho(\mathbf{v}^{(i)})$ .

Algorithm 1 presents a high-level CEGAR loop for checking whether  $M \models \Phi$ . It is parameterized by three functions. The **Abstract** function produces an initial *sound abstraction* of  $M$ . The **Prove** function checks whether  $M' \models \Phi$ . If so (i.e., the property  $\Phi$  holds for  $M'$ ), it returns with *proven* set to true. Otherwise, it returns an assignment  $\alpha$  which constitutes a counter-example. The final function is **Refine**, which takes  $M$  and  $M'$ , the property  $P$ , and the counterexample  $\alpha$  for  $M'$  as inputs. Its job is to refine the abstraction until  $\alpha$  is no longer a counter-example. If it succeeds, it returns a new sound abstraction  $M'$ . It fails if  $\alpha$  is an actual counter-example for the original  $M$ . In this case, it sets the return value *refined* to false. Throughout its execution, the algorithm maintains

	Case 1	Case 2	Case 3	Case 4	Case 5
					
	$l < \eta, u > \eta$ $\rho''(p) > 0$	$l < \eta, u > \eta$ $\rho''(p) = 0$	$l < \eta, u > \eta$ $\rho''(p) < 0$	$l > \eta \vee u < \eta$ $\rho''(p) \leq 0$	$l > \eta \vee u < \eta$ $\rho''(p) > 0$
$\beta$	$\rho'(p)$	$\rho'(p)$	$\frac{\rho(l) - k \cdot l - \rho(p)}{\eta - p}$ where $k = \min(\rho'(l), \rho'(u))$	$\frac{\rho(p) - \rho(l)}{p - l}$	$\rho'(p)$
$\gamma$	$\min(\rho'(l), \rho'(u))$	$\frac{\rho(p) - \rho(u)}{p - u}$	$\frac{\rho(p) - \rho(u)}{p - u}$	$\frac{\rho(p) - \rho(u)}{p - u}$	$\rho'(p)$

**Table 1:** Choice of the slopes of the piece-wise linear abstraction refinement.

a sound abstraction of  $M$  and checks whether the property  $\Phi$  holds on the abstraction. If a counter-example  $\alpha$  is found such that  $M'[\alpha] \models \neg\Phi$ , the algorithm uses it to refine the abstraction so that  $\alpha$  is no longer a counter-example. The following theorem follows directly from Def. 4.1:

**Theorem 4.2** (CEGAR is sound). *Alg. 1 returns true only if  $M \models \Phi$ .*

#### 4.1 Choice of the underlying verifier and initial abstraction

The Prove function can be instantiated with an existing DNN verifier. The verifier is required to (1) handle piecewise-linear constraints; and (2) produce counter-examples. There are many existing verifiers that meet these requirements [14, 31, 44, 51]. To ensure that these two requirements are sufficient, we also require that  $\phi'_{\text{aff}}$  and  $\phi'_\rho$  only contain linear and piecewise-linear formulas.

The Abstract function creates an initial abstraction. For simplicity, we assume that all piecewise-linear formulas are unchanged by the abstraction function. For sigmoid activations, we use piecewise-linear over-approximations. In principle, any sound piecewise-linear over-approximation of the sigmoid function could be used. One approach is to use a fine-grained over-approximation with piecewise-linear bounds [68]. While this approach can arbitrarily reduce over-approximation error, it might easily lead to an explosion of the state space when reasoning about generative models due to the large number of transcendental activations (equal to the dimension of the generated image) present in the system. One key insight of CEGAR is that it is often the case that most of the complexity of the original system is unnecessary for proving the property and eagerly adding it upfront only increases the computational cost. We thus propose starting with a coarse (e.g., convex) over-approximation and only refining with additional piecewise-linear constraints when necessary. Suitable candidates for the initial abstraction of a sigmoid function include the abstraction proposed in [18, 31, 34, 51, 64], which considers the convex relaxation of the sigmoid activation.

#### 4.2 Abstraction Refinement for the sigmoid activation function.

We now focus on the problem of abstraction refinement for models with sigmoid activation functions. Suppose that an assignment  $\alpha$  is found by Prove such that  $M'[\alpha] \models \neg\Phi$ , but for some neuron with sigmoid activation  $\rho$ , represented by variables  $(v, \hat{v})$ ,  $\alpha(\hat{v}) \neq \rho(\alpha(v))$ . The goal is to refine the abstraction  $M'$ , so that  $\alpha$  is no longer a counter-example for the refined model. Here we present a refinement strategy that is applicable to *any* sound abstraction of sigmoid functions. We propose using two linear segments to exclude spurious counter-examples. The key insight is that this is always sufficient for ruling out any counter-example. We assume that  $\phi'_{\text{aff}}$  includes upper and lower bounds for each variable  $v$  that is an input to a sigmoid function. In practice, bounds can be computed with bound-propagation techniques [31, 34, 35].

**Lemma 4.3.** *Given an interval  $(l, u)$ , a sigmoid function  $\rho$ , and a point  $(p, q) \in \mathbb{R}^2$ , where  $p \in (l, u)$  and  $q \neq \rho(p)$ , there exists a piecewise-linear function  $h : \mathbb{R} \mapsto \mathbb{R}$  that 1) has two linear segments; 2) evaluates to  $\rho(p)$  at  $p$ ; and 3) separates  $\{(p, q)\}$  and  $\{(x, y) \mid x \in (l, u) \wedge y = \rho(x)\}$ .*

---

**Algorithm 2**  $\text{Refine}(M' := \langle \mathcal{V}', \mathcal{X}, \mathcal{Y}, \phi'_{\text{aff}}, \phi'_{\rho} \rangle, \Phi, \alpha : \mathcal{V} \mapsto \mathbb{R})$ .

---

```

1:  $refined \leftarrow 0$ 
2: for  $(v, \hat{v}) \in \text{AllSigmoid}(\mathcal{V}')$  do
3:   if  $\alpha(\hat{v}) = \rho(\alpha(v))$  then continue ▷ Skip satisfied activations.
4:    $refined \leftarrow refined + 1$ 
5:    $\beta, \gamma \leftarrow \text{getSlopes}(l(v), u(v), \alpha(v), \alpha(\hat{v}))$  ▷ Compute slopes.
6:    $\phi'_{\rho} \leftarrow \phi'_{\rho} \cup \text{addPLBound}(\beta, \gamma, v, \hat{v}, \alpha)$  ▷ Refine the abstraction.
7:   if  $\text{stopCondition}(refined)$  then break ▷ Check termination condition.
8: return  $\langle \mathcal{V}', \mathcal{X}, \mathcal{Y}, \phi'_{\text{aff}}, \phi'_{\rho} \rangle, refined > 0$ 

```

---

Leveraging this observation, given a point  $(p, q) = (\alpha(v), \alpha(\hat{v}))$ , we can construct a piecewise-linear function  $h$  of the following form:

$$h(x) = \rho(p) + \begin{cases} \beta(x - p) & \text{if } x \leq p \\ \gamma(x - p) & \text{if } x > p \end{cases}$$

that separates the counter-example and the sigmoid function. If  $q > \rho(p)$ , we add the formula  $\hat{v} \leq h(v)$  to the abstraction. And if  $q < \rho(p)$ , we add  $\hat{v} \geq h(v)$ .

The values for the slopes  $\beta$  and  $\gamma$  should ideally be chosen to minimize the over-approximation error while maintaining soundness. Additionally, they should be easily computable. Table. 1 presents a general recipe for choosing  $\beta$  and  $\gamma$  when the spurious counter-example point is below the sigmoid function. Choosing  $\beta$  and  $\gamma$  when the counter-example is above the sigmoid function is symmetric (details are shown in App. A).  $\eta$  denotes the inflection point of the sigmoid function.

Note that in case 5,  $\beta$  is the same as  $\gamma$ , meaning that a linear bound (the tangent line to  $\rho$  at  $p$ ) suffices to exclude the counter-example. In terms of optimality, all but the  $\gamma$  value in case 1 and the  $\beta$  value in case 3 maximally reduce the over-approximation error among all valid slopes at  $(p, \rho(p))$ . In those two cases, linear or binary search techniques [34, 51] could be applied to compute better slopes, but the formulas shown give the best approximations we could find without using search.

**Lemma 4.4** (Soundness of slopes). *Choosing  $\beta$  and  $\gamma$  using the recipe shown in Table 1 results in a piecewise-linear function  $h$  that satisfies the conditions of Lemma 4.3.*

An instantiation of the `Refine` function for neural networks with sigmoid activation is shown in Alg. 2. It iterates through each sigmoid activation function. For the ones that are violated by the current assignment, the algorithm computes the slopes following the strategy outlined above with the `getSlopes` function and adds the corresponding piecewise-linear bounds (e.g.,  $\hat{v} \geq h(v)$ ) with the `addPLBound` function. Finally, we also allow the flexibility to terminate the refinement early with a customized `stopCondition` function. This is likely desirable in practice, as introducing a piecewise-linear bound for each violated activation might be too aggressive. Furthermore, adding a single piecewise-linear bound already suffices to exclude  $\alpha$ . We use an adaptive stopping strategy where we allow at most  $m$  piecewise-linear bounds to be added in the first invocation of Alg. 2. And then, in each subsequent round, this number is increased by a factor  $k$ . For our evaluation, below, we used  $m = 30$  and  $k = 2$ , which were the values that performed best in an empirical analysis.

**Theorem 4.5** (Soundness of refinement). *Given a sound abstraction  $M'$  of tuple  $M$ , a property  $\Phi$ , and a spurious counter-example  $\alpha$  s.t.  $M'[\alpha] \models \neg\Phi$  and  $M[\alpha] \models \Phi$ , Alg. 2 produces a sound abstraction of  $M$ ,  $M''$ , s.t.  $M''[\alpha] \models \Phi$ .*

## 5 Experimental evaluation

In this section, we evaluate the performance of our proposed verification framework. We begin by comparing our method with existing approaches on two real-world distribution shifts (§5.1). Next, we benchmark the performance of our verifier on a range of challenging distribution shifts (§ 5.2). Finally, we use our method to show that robust training tends to result in higher levels of certified robustness against distribution shifts (§ 5.3).

**Datasets.** We consider a diverse array of distribution shifts on the MNIST [69] and CIFAR-10 [70] datasets. The code used to generate the perturbations is adapted from [10].

Dataset	Gen.	Class.	DP	DP+BaB		DP+BaB+CEGAR		
			$\delta$	$\delta$	time(s)	$\delta$	time(s)	# ref.
MNIST	MLP_GEN <sub>1</sub>	MLP_CLASS <sub>1</sub>	0.104 ± 0.041	0.139 ± 0.058	7.8	<b>0.157</b> ± 0.057	84.1	1.5 ± 1.1
	MLP_GEN <sub>2</sub>	MLP_CLASS <sub>1</sub>	0.08 ± 0.035	0.106 ± 0.049	20.4	<b>0.118</b> ± 0.049	114.8	1.0 ± 1.1
	MLP_GEN <sub>1</sub>	MLP_CLASS <sub>2</sub>	0.102 ± 0.044	0.136 ± 0.061	16.4	<b>0.15</b> ± 0.059	120.6	1.2 ± 1.2
	MLP_GEN <sub>2</sub>	MLP_CLASS <sub>2</sub>	0.081 ± 0.037	0.112 ± 0.049	60.8	<b>0.121</b> ± 0.049	191.6	0.8 ± 1.1
	MLP_GEN <sub>1</sub>	MLP_CLASS <sub>3</sub>	0.099 ± 0.041	0.135 ± 0.062	41.3	<b>0.146</b> ± 0.059	186.9	1.0 ± 1.1
	MLP_GEN <sub>2</sub>	MLP_CLASS <sub>3</sub>	0.082 ± 0.036	0.116 ± 0.044	75.7	<b>0.122</b> ± 0.041	163.3	0.6 ± 1.0
CIFAR	CONV_GEN <sub>1</sub>	CONV_CLASS <sub>1</sub>	0.219 ± 0.112	0.273 ± 0.153	33.5	<b>0.287</b> ± 0.148	140.8	4.5 ± 9.2
	CONV_GEN <sub>2</sub>	CONV_CLASS <sub>1</sub>	0.131 ± 0.094	0.18 ± 0.117	13.7	<b>0.194</b> ± 0.115	112.5	3.1 ± 6.0
	CONV_GEN <sub>1</sub>	CONV_CLASS <sub>2</sub>	0.176 ± 0.108	0.242 ± 0.14	16.0	<b>0.253</b> ± 0.136	57.7	1.6 ± 2.4
	CONV_GEN <sub>2</sub>	CONV_CLASS <sub>2</sub>	0.12 ± 0.077	0.154 ± 0.087	7.9	<b>0.172</b> ± 0.085	140.2	3.3 ± 4.2

**Table 2:** Evaluation results of three solver configurations.

**Training algorithms.** For each distribution shift we consider, we train a CVAE using the framework outlined in [9]. For each dataset, the number of sigmoid activations used in the CVAE is the same as the (flattened) output dimension; that is, we use 784 ( $28 \times 28$ ) sigmoids for MNIST and 3072 ( $3 \times 32 \times 32$ ) sigmoids for CIFAR-10. Throughout this section, we use various training algorithms, including empirical risk minimization (ERM) [71], invariant risk minimization (IRM) [72], projected gradient descent (PGD) [2], and model-based dataset augmentation (MDA) [8].

**Implementation details.** We use the DeepPoly [31] method, which over-approximates the sigmoid output with two linear inequalities (an upper and a lower bound), to obtain an initial abstraction (the **Abstract** function in Alg. 1) for each sigmoid and instantiate the **Prove** function with the Marabou neural network verification tool. [14]<sup>2</sup> All experiments are run on a cluster equipped with Intel Xeon E5-2637 v4 CPUs running Ubuntu 16.04 with 8 threads and 32GB memory.

## 5.1 Comparison of verification performance

We first compare the performance of our proposed CEGAR procedure to other baseline verifiers that do not perform abstraction refinement. To do so, we compare the largest perturbation  $\delta$  in the latent space of generative models  $G$  that each verifier can certify. In our comparison, we consider three distinct configurations: (1) DP, which runs the DeepPoly abstract interpretation procedure without any search; (2) DP+BaB, which runs a branch-and-bound procedure (Marabou) on an encoding where each sigmoid is abstracted with the DeepPoly linear bounds and the other parts are precisely encoded; and (3) DP+BaB+CEGAR, which is the CEGAR method proposed in this work.<sup>3</sup> For each verifier, we perform a linear search for the largest perturbation bound each configuration can certify. Specifically, starting from  $\delta = 0$ , we repeatedly increase  $\delta$  by 0.02 and check whether the configuration can prove robustness with respect to  $\mathcal{S}(x)$  within a given time budget (20 minutes). The process terminates when a verifier fails to prove or disprove a given specification.

For this experiment, we consider the *shear* distribution shift on MNIST and the *fog* distribution shift on the CIFAR-10 dataset (see Figure 2). All classifiers are trained using ERM. To provide a thorough evaluation, we consider several generator and classifier architectures; details can be found in App. D. Our results are enumerated in Table 2, which shows the mean and standard deviation of the largest  $\delta$  each configuration is able to prove for the first 100 correctly classified test images. We also report the average runtime on the largest  $\delta$  proven robust by DP+BaB and DP+BaB+CEGAR, as well as the average number of abstraction refinement rounds by DP+BaB+CEGAR on those  $\delta$  values. Across all configurations, our proposed technique effectively improves the verifiable perturbation bound with moderate runtime overhead. This suggests that the counter-example guided abstraction refinement scheme can successfully boost the precision when reasoning about sigmoid activations by leveraging existing verifiers. Further comparison of our techniques against existing verifiers on adversarial robustness verification of sigmoid-based classifiers are provided in App. E.

## 5.2 Benchmarking our approach on an array of real-world distribution shifts

<sup>2</sup>We note that our framework is general and can be used with other abstractions and solvers.

<sup>3</sup>We also tried eagerly abstracting the sigmoid with fine-grained piecewise-linear bounds, but the resulting configuration performs much worse than a lazy approach in terms of runtime. Details are shown in App. E



We next use our proposed verification procedure to evaluate the robustness of classifiers trained using ERM against a wide range of distribution shifts. We select the first 100 correctly classified test images from the respective dataset for each perturbation and verify the robustness of the classifier against the perturbation set. Three values of the perturbation variable  $\delta$  are considered: 0.1, 0.2, and 0.5. The architectures we consider for MNIST are MLP\_GEN<sub>2</sub> and MLP\_CLASS<sub>3</sub>. For CIFAR-10 we use CONV\_GEN<sub>2</sub> and CONV\_CLASS<sub>2</sub>. The verification results are shown in Figure 4. The “robust” columns show the number of instances that our verification procedure is able to certify within a 20 minute timeout. As one would expect, the robustness of each classifier deteriorates as the perturbation budget  $\delta$  increases. For instance, for the shear transformation, the classifier is robust on 76 out of the 100 instances when  $\delta = 0.1$ , but is only certified robust on 4 instances when  $\delta$  increases to 0.2. Information like this could help system developers to identify perturbation classes for which the network is especially vulnerable and potentially retrain the network accordingly.

Dataset	Perturbation	$\delta = 0.1$		$\delta = 0.2$		$\delta = 0.5$	
		robust	time(s)	robust	time(s)	robust	time(s)
MNIST	brightness	99	3.4	96	5.0	89	13.7
	rotation	51	38.6	11	80.1	1	177.9
	gaussian-blur	86	4.7	79	10.8	65	36.5
	shear	76	21.4	4	102.6	0	135.6
	contrast	90	5.9	85	11.1	74	51.0
	scale	95	8.0	84	30.8	3	122.7
CIFAR10	brightness	97	3.2	96	5.2	86	18.5
	contrast	97	3.0	95	4.6	77	40.0
	fog	84	34.3	64	69.1	11	256.0
	gaussian-blur	100	2.9	99	3	94	10.7

Figure 4: Robustness of ERM against different perturbations.

### 5.3 Verification for various robust training algorithms

Finally, we compare the robustness and accuracy of classifiers trained using ERM, IRM, PGD, and MDA against the shear distribution shifts on the MNIST dataset. To this end, we measure the accuracy on the entire test set under the learned perturbation generative models. For each classifier, we then select the first 500 correctly classified images in its dataset and verify the targeted robustness of the classifier against the perturbation. The architectures we use are MLP\_GEN<sub>2</sub> and MLP\_CLASS<sub>3</sub>.

Dataset	Train. Alg.	Test set Accuracy %		Certified Robust %	
		Standard	Generative	$\delta = 0.05$	$\delta = 0.1$
MNIST	ERM	97.9	71.6	73.2	62.4
	IRM	97.8	78.7	91.4	37.0
	PGD	97.0	79.5	91.0	73.8
	MDA	97.2	96.5	97.2	86.6

Figure 5: Test set accuracy and verification accuracy

Accuracy and robustness results are presented in Figure 5. Interestingly, MDA, which is perturbation-aware, outperforms the other three perturbation-agnostic training methods, on both test accuracy and robustness, suggesting that knowing what type of perturbation to anticipate is highly useful. Notice that accuracy on the perturbation set is not necessarily a good proxy for robustness: while the IRM-trained classifier has similar accuracy as the PGD-trained classifier, the former is significantly less robust on the perturbation set with  $\delta = 0.1$ . This further supports the need for including formal verification in the systematic evaluation of neural networks and training algorithms.

## 6 Related Work

**Beyond norm-bounded perturbations.** While the literature concerning DNN verification has predominantly focused on robustness against norm-bounded perturbations, some work has considered other forms of robustness, e.g., against geometric transformations of data [53–55]. However, the perturbations considered are hand-crafted and can be analytically defined by simple models. In contrast, our goal is to verify against real-world distribution shifts that are defined via the output set of a generative model. Our approach also complements recent work which has sought to incorporate neural symbolic components into formal specifications [63]. Our main contribution with respect to that work is to propose the use of deep generative models in such specifications and to design new tools which can handle the unique technical challenges that arise from this setting.

**Existing verification approaches.** Existing DNN verification algorithms broadly fall into one of two categories: search-based methods [13–30] and abstraction-based methods [31–50]. While several existing solvers can handle sigmoid activation functions [18, 31, 34, 51, 64], they rely on one-shot abstraction and lack a refinement scheme for continuous progress. On the other hand, a separate

line of work has shown that verifying DNNs containing a single layer of logistic activations is decidable [73], but the decision procedure proposed in this work is computationally prohibitive. To overcome these limitations, we propose a meta-algorithm inspired by counter-example-guided abstraction refinement [66] that leverages existing verifiers to solve increasingly refined abstractions.

**Verification against distribution shifts.** The authors of [9] also considered the task of evaluating DNN robustness to real-world distribution shifts; in particular, the approach used in [9] relies on randomized smoothing [74]. This scheme provides *probabilistic* guarantees on robustness, whereas our approach (as well as the aforementioned approaches) provides *deterministic* guarantees. In a separate line of work, several authors have sought to perform verification of deep generative models [56, 61]. However, each of these works assumes that generative models are piece-wise linear functions, which precludes the use of state-of-the-art models.

## 7 Conclusion

In this paper, we presented a framework for certifying robustness against real-world distribution shifts. We proposed using provably trained deep generative models to define formal specifications and a new abstraction-refinement algorithm for verifying them. Experiments show that our method can certify against larger perturbation sets than previous techniques.

**Limitations.** We now discuss some limitations of our framework. First, like many verification tools, the classifier architectures that our approach can verify are smaller than popular architectures such as ResNet [75] and DenseNet [76]. This stems from the limited capacity of existing DNN verification tools for piecewise-linear functions, which we invoke in the CEGAR loop. Given the rapid growth of the DNN verification community, we are optimistic that the scalability of verifiers will continue to grow rapidly, enabling their use on larger and larger networks. Another limitation is that the quality of our neural symbolic specification is determined by how well the generative model captures real-world distribution shifts. The mismatch between formal specification and reality is in fact common (and often unavoidable) in formal verification. And while [9] shows that under favorable conditions, CVAEs can capture distribution shifts, these assumptions may not hold in practice. For this reason, we envision that in addition to these theoretical results, a necessary future direction will be to involve humans in the verification loop to validate the shifts captured by generative models and the produced counterexamples. This resembles how verification teams work closely with product teams to continually re-evaluate and adjust the specifications in existing industrial settings.

## References

- [1] Ian J Goodfellow, Jonathon Shlens, and Christian Szegedy. Explaining and harnessing adversarial examples. *arXiv preprint arXiv:1412.6572*, 2014.
- [2] Aleksander Madry, Aleksandar Makelov, Ludwig Schmidt, Dimitris Tsipras, and Adrian Vladu. Towards deep learning models resistant to adversarial attacks. *arXiv preprint arXiv:1706.06083*, 2017.
- [3] Eric Wong and Zico Kolter. Provable defenses against adversarial examples via the convex outer adversarial polytope. In *International Conference on Machine Learning*, pages 5286–5295. PMLR, 2018.
- [4] Hongyang Zhang, Yaodong Yu, Jiantao Jiao, Eric Xing, Laurent El Ghaoui, and Michael Jordan. Theoretically principled trade-off between robustness and accuracy. In *International conference on machine learning*, pages 7472–7482. PMLR, 2019.
- [5] Harini Kannan, Alexey Kurakin, and Ian Goodfellow. Adversarial logit pairing. *arXiv preprint arXiv:1803.06373*, 2018.
- [6] Seyed-Mohsen Moosavi-Dezfooli, Alhussein Fawzi, and Pascal Frossard. Deepfool: a simple and accurate method to fool deep neural networks. In *Proceedings of the IEEE conference on computer vision and pattern recognition*, pages 2574–2582, 2016.
- [7] Alexander Robey, Luiz Chamon, George J Pappas, Hamed Hassani, and Alejandro Ribeiro. Adversarial robustness with semi-infinite constrained learning. *Advances in Neural Information Processing Systems*, 34:6198–6215, 2021.
- [8] Alexander Robey, Hamed Hassani, and George J Pappas. Model-based robust deep learning. *arXiv preprint arXiv:2005.10247*, 2020.
- [9] Eric Wong and J Zico Kolter. Learning perturbation sets for robust machine learning. *arXiv preprint arXiv:2007.08450*, 2020.
- [10] Dan Hendrycks and Thomas Dietterich. Benchmarking neural network robustness to common corruptions and perturbations. *arXiv preprint arXiv:1903.12261*, 2019.
- [11] Dan Hendrycks, Steven Basart, Norman Mu, Saurav Kadavath, Frank Wang, Evan Dorundo, Rahul Desai, Tyler Zhu, Samyak Parajuli, Mike Guo, et al. The many faces of robustness: A critical analysis of out-of-distribution generalization. *arXiv preprint arXiv:2006.16241*, 2020.
- [12] Pang Wei Koh, Shiori Sagawa, Henrik Marklund, Sang Michael Xie, Marvin Zhang, Akshay Balsubramani, Weihua Hu, Michihiro Yasunaga, Richard Lanus Phillips, Irena Gao, et al. Wilds: A benchmark of in-the-wild distribution shifts. *arXiv preprint arXiv:2012.07421*, 2020.
- [13] G. Katz, C. Barrett, D. Dill, K. Julian, and M. Kochenderfer. Reluplex: An Efficient SMT Solver for Verifying Deep Neural Networks. In *Proc. 29th Int. Conf. on Computer Aided Verification (CAV)*, pages 97–117, 2017.
- [14] Guy Katz, Derek A Huang, Duligur Ibeling, Kyle Julian, Christopher Lazarus, Rachel Lim, Parth Shah, Shantanu Thakoor, Haoze Wu, Aleksandar Zeljić, et al. The marabou framework for verification and analysis of deep neural networks. In *International Conference on Computer Aided Verification*, pages 443–452, 2019.
- [15] Vincent Tjeng, Kai Xiao, and Russ Tedrake. Evaluating robustness of neural networks with mixed integer programming. *arXiv preprint arXiv:1711.07356*, 2017.
- [16] Alessandro De Palma, Harkirat Singh Behl, Rudy Bunel, Philip HS Torr, and M Pawan Kumar. Scaling the convex barrier with active sets. *arXiv preprint arXiv:2101.05844*, 2021.
- [17] Rudy Bunel, Jingyue Lu, Ilker Turkaslan, Pushmeet Kohli, P Torr, and P Mudigonda. Branch and bound for piecewise linear neural network verification. *Journal of Machine Learning Research*, 21(2020), 2020.

- [18] Kaidi Xu, Huan Zhang, Shiqi Wang, Yihan Wang, Suman Jana, Xue Lin, and Cho-Jui Hsieh. Fast and complete: Enabling complete neural network verification with rapid and massively parallel incomplete verifiers. *arXiv preprint arXiv:2011.13824*, 2020.
- [19] Rüdiger Ehlers. Formal verification of piece-wise linear feed-forward neural networks. *CoRR*, abs/1705.01320, 2017.
- [20] Elena Botoeva, Panagiotis Kouvaros, Jan Kronqvist, Alessio Lomuscio, and Ruth Misener. Efficient verification of relu-based neural networks via dependency analysis. In *Proceedings of the AAAI Conference on Artificial Intelligence*, volume 34, pages 3291–3299, 2020.
- [21] Greg Anderson, Shankara Pailoor, Isil Dillig, and Swarat Chaudhuri. Optimization and abstraction: A synergistic approach for analyzing neural network robustness. In *Proc. Programming Language Design and Implementation (PLDI)*, page 731–744, 2019.
- [22] Haitham Khedr, James Ferlez, and Yasser Shoukry. Peregrinn: Penalized-relaxation greedy neural network verifier. *arXiv preprint arXiv:2006.10864*, 2020.
- [23] Matteo Fischetti and Jason Jo. Deep neural networks as 0-1 mixed integer linear programs: A feasibility study. *CoRR*, abs/1712.06174, 2017.
- [24] Rudy Bunel, Alessandro De Palma, Alban Desmaison, Krishnamurthy Dvijotham, Pushmeet Kohli, Philip Torr, and M Pawan Kumar. Lagrangian decomposition for neural network verification. In *Conference on Uncertainty in Artificial Intelligence*, pages 370–379. PMLR, 2020.
- [25] Krishnamurthy Dvijotham, Robert Stanforth, Sven Gowal, Timothy A Mann, and Pushmeet Kohli. A dual approach to scalable verification of deep networks. In *UAI*, volume 1, page 3, 2018.
- [26] Krishnamurthy Dvijotham, Robert Stanforth, Sven Gowal, Chongli Qin, Soham De, and Pushmeet Kohli. Efficient neural network verification with exactness characterization. In *Uncertainty in Artificial Intelligence*, pages 497–507. PMLR, 2020.
- [27] Haoze Wu, Aleksandar Zeljić, Guy Katz, and Clark Barrett. Efficient neural network analysis with sum-of-infeasibilities. In *International Conference on Tools and Algorithms for the Construction and Analysis of Systems*, pages 143–163. Springer, 2022.
- [28] Claudio Ferrari, Mark Niklas Muller, Nikola Jovanovic, and Martin Vechev. Complete verification via multi-neuron relaxation guided branch-and-bound. *arXiv preprint arXiv:2205.00263*, 2022.
- [29] Hoang-Dung Tran, Stanley Bak, Weiming Xiang, and Taylor T Johnson. Verification of deep convolutional neural networks using imagestars. In *International Conference on Computer Aided Verification*, pages 18–42. Springer, 2020.
- [30] Xiaowei Huang, Marta Kwiatkowska, Sen Wang, and Min Wu. Safety verification of deep neural networks. In *CAV*, 2017.
- [31] Gagandeep Singh, Timon Gehr, Markus Püschel, and Martin Vechev. An abstract domain for certifying neural networks. *Proceedings of the ACM on Programming Languages*, 3(POPL):1–30, 2019.
- [32] Gagandeep Singh, Rupanshu Ganvir, Markus Püschel, and Martin Vechev. Beyond the single neuron convex barrier for neural network certification. *Advances in Neural Information Processing Systems*, 32:15098–15109, 2019.
- [33] Zhaoyang Lyu, Ching-Yun Ko, Zhifeng Kong, Ngai Wong, Dahua Lin, and Luca Daniel. Fastened crown: Tightened neural network robustness certificates. In *Proceedings of the AAAI Conference on Artificial Intelligence*, volume 34, pages 5037–5044, 2020.
- [34] Huan Zhang, Tsui-Wei Weng, Pin-Yu Chen, Cho-Jui Hsieh, and Luca Daniel. Efficient neural network robustness certification with general activation functions. *arXiv preprint arXiv:1811.00866*, 2018.

- [35] Shiqi Wang, Kexin Pei, Justin Whitehouse, Junfeng Yang, and Suman Jana. Formal security analysis of neural networks using symbolic intervals. In *27th USENIX Security Symposium, USENIX Security 2018, Baltimore, MD, USA, August 15-17, 2018*, pages 1599–1614, 2018.
- [36] Shiqi Wang, Kexin Pei, Justin Whitehouse, Junfeng Yang, and Suman Jana. Efficient formal safety analysis of neural networks. In *Advances in Neural Information Processing Systems 31: Annual Conference on Neural Information Processing Systems 2018, NeurIPS 2018, 3-8 December 2018, Montréal, Canada*, pages 6369–6379, 2018.
- [37] Souradeep Dutta, Susmit Jha, Sriram Sankaranarayanan, and Ashish Tiwari. Output range analysis for deep feedforward neural networks. In *NASA Formal Methods - 10th International Symposium, NFM 2018, Newport News, VA, USA, April 17-19, 2018, Proceedings*, 2018.
- [38] Lily Weng, Huan Zhang, Hongge Chen, Zhao Song, Cho-Jui Hsieh, Luca Daniel, Duane Boning, and Inderjit Dhillon. Towards fast computation of certified robustness for relu networks. In *International Conference on Machine Learning*, pages 5276–5285. PMLR, 2018.
- [39] Hadi Salman, Greg Yang, Huan Zhang, Cho-Jui Hsieh, and Pengchuan Zhang. A convex relaxation barrier to tight robustness verification of neural networks. *arXiv preprint arXiv:1902.08722*, 2019.
- [40] Christian Tjandraatmadja, Ross Anderson, Joey Huchette, Will Ma, Krunal Patel, and Juan Pablo Vielma. The convex relaxation barrier, revisited: Tightened single-neuron relaxations for neural network verification. *arXiv preprint arXiv:2006.14076*, 2020.
- [41] Aditi Raghunathan, Jacob Steinhardt, and Percy Liang. Semidefinite relaxations for certifying robustness to adversarial examples. *arXiv preprint arXiv:1811.01057*, 2018.
- [42] Weiming Xiang, Hoang-Dung Tran, and Taylor T Johnson. Output reachable set estimation and verification for multilayer neural networks. *IEEE transactions on neural networks and learning systems*, 29(11):5777–5783, 2018.
- [43] Timon Gehr, Matthew Mirman, Dana Drachler-Cohen, Petar Tsankov, Swarat Chaudhuri, and Martin T. Vechev. AI2: safety and robustness certification of neural networks with abstract interpretation. In *2018 IEEE Symposium on Security and Privacy, SP 2018, Proceedings, 21-23 May 2018, San Francisco, California, USA*, pages 3–18, 2018.
- [44] Shiqi Wang, Huan Zhang, Kaidi Xu, Xue Lin, Suman Jana, Cho-Jui Hsieh, and J Zico Kolter. Beta-crown: Efficient bound propagation with per-neuron split constraints for complete and incomplete neural network verification. *arXiv preprint arXiv:2103.06624*, 2021.
- [45] Gagandeep Singh, Timon Gehr, Markus Püschel, and Martin Vechev. Boosting robustness certification of neural networks. In *International Conference on Learning Representations*, 2019.
- [46] Akhilan Boopathy, Tsui-Wei Weng, Pin-Yu Chen, Sijia Liu, and Luca Daniel. Cnn-cert: An efficient framework for certifying robustness of convolutional neural networks. In *Proceedings of the AAAI Conference on Artificial Intelligence*, volume 33, pages 3240–3247, 2019.
- [47] Gagandeep Singh, Timon Gehr, Matthew Mirman, Markus Püschel, and Martin Vechev. Fast and effective robustness certification. *Advances in Neural Information Processing Systems*, 31:10802–10813, 2018.
- [48] Mark Niklas Müller, Gleb Makarchuk, Gagandeep Singh, Markus Püschel, and Martin Vechev. Prima: general and precise neural network certification via scalable convex hull approximations. *Proceedings of the ACM on Programming Languages*, 6(POPL):1–33, 2022.
- [49] Yizhak Yisrael Elboher, Justin Gottschlich, and Guy Katz. An abstraction-based framework for neural network verification. In *International Conference on Computer Aided Verification*, pages 43–65. Springer, 2020.
- [50] Wonryong Ryou, Jiayu Chen, Mislav Balunovic, Gagandeep Singh, Andrei Dan, and Martin Vechev. Scalable polyhedral verification of recurrent neural networks. In *International Conference on Computer Aided Verification*, pages 225–248. Springer, 2021.

- [51] Patrick Henriksen and Alessio Lomuscio. Efficient neural network verification via adaptive refinement and adversarial search. In *ECAI 2020*, pages 2513–2520. IOS Press, 2020.
- [52] Battista Biggio, Iginio Corona, Davide Maiorca, Blaine Nelson, Nedim Šrđić, Pavel Laskov, Giorgio Giacinto, and Fabio Roli. Evasion attacks against machine learning at test time. In *Joint European conference on machine learning and knowledge discovery in databases*, pages 387–402. Springer, 2013.
- [53] Mislav Balunović, Maximilian Baader, Gagandeep Singh, Timon Gehr, and Martin Vechev. Certifying geometric robustness of neural networks. *Advances in Neural Information Processing Systems* 32, 2019.
- [54] Colin Paterson, Haoze Wu, John Grese, Radu Calinescu, Corina S Pasareanu, and Clark Barrett. Deepcert: Verification of contextually relevant robustness for neural network image classifiers. *arXiv preprint arXiv:2103.01629*, 2021.
- [55] Jeet Mohapatra, Pin-Yu Chen, Sijia Liu, Luca Daniel, et al. Towards verifying robustness of neural networks against semantic perturbations. *arXiv preprint arXiv:1912.09533*, 2019.
- [56] Sydney M Katz, Anthony L Corso, Christopher A Strong, and Mykel J Kochenderfer. Verification of image-based neural network controllers using generative models. In *2021 IEEE/AIAA 40th Digital Avionics Systems Conference (DASC)*, pages 1–10. IEEE, 2021.
- [57] Sven Gowal, Chongli Qin, Po-Sen Huang, Taylan Cemgil, Krishnamurthy Dvijotham, Timothy Mann, and Pushmeet Kohli. Achieving robustness in the wild via adversarial mixing with disentangled representations. In *Proceedings of the IEEE/CVF Conference on Computer Vision and Pattern Recognition*, pages 1211–1220, 2020.
- [58] Alexander Robey, George J Pappas, and Hamed Hassani. Model-based domain generalization. *arXiv preprint arXiv:2102.11436*, 2021.
- [59] Yuning You, Tianlong Chen, Yang Shen, and Zhangyang Wang. Graph contrastive learning automated. In *International Conference on Machine Learning*, pages 12121–12132. PMLR, 2021.
- [60] Vishnu M Bashyam, Jimit Doshi, Guray Erus, Dhivya Srinivasan, Ahmed Abdulkadir, Ashish Singh, Mohamad Habes, Yong Fan, Colin L Masters, Paul Maruff, et al. Deep generative medical image harmonization for improving cross-site generalization in deep learning predictors. *Journal of Magnetic Resonance Imaging*, 55(3):908–916, 2022.
- [61] Matthew Mirman, Alexander Hägele, Pavol Bielik, Timon Gehr, and Martin Vechev. Robustness certification with generative models. In *Proceedings of the 42nd ACM SIGPLAN International Conference on Programming Language Design and Implementation*, pages 1141–1154, 2021.
- [62] Xun Huang, Ming-Yu Liu, Serge Belongie, and Jan Kautz. Multimodal unsupervised image-to-image translation. In *Proceedings of the European conference on computer vision (ECCV)*, pages 172–189, 2018.
- [63] Xuan Xie, Kristian Kersting, and Daniel Neider. Neuro-symbolic verification of deep neural networks. 2022.
- [64] Mark Niklas Müller, Gleb Makarchuk, Gagandeep Singh, Markus Püschel, and Martin Vechev. Precise multi-neuron abstractions for neural network certification. *arXiv preprint arXiv:2103.03638*, 2021.
- [65] Kaidi Xu, Zhouxing Shi, Huan Zhang, Yihan Wang, Kai-Wei Chang, Minlie Huang, Bhavya Kailkhura, Xue Lin, and Cho-Jui Hsieh. Automatic perturbation analysis for scalable certified robustness and beyond. *Advances in Neural Information Processing Systems*, 33:1129–1141, 2020.
- [66] Edmund Clarke, Orna Grumberg, Somesh Jha, Yuan Lu, and Helmut Veith. Counterexample-guided abstraction refinement. In *International Conference on Computer Aided Verification*, pages 154–169. Springer, 2000.

- [67] Makai Mann, Ahmed Irfan, Alberto Griggio, Oded Padon, and Clark Barrett. Counterexample-guided prophecy for model checking modulo the theory of arrays. In *International Conference on Tools and Algorithms for the Construction and Analysis of Systems*, pages 113–132. Springer, 2021.
- [68] Chelsea Sidrane, Amir Maleki, Ahmed Irfan, and Mykel J Kochenderfer. Overt: An algorithm for safety verification of neural network control policies for nonlinear systems. *Journal of Machine Learning Research*, 23(117):1–45, 2022.
- [69] Yann LeCun, Léon Bottou, Yoshua Bengio, and Patrick Haffner. Gradient-based learning applied to document recognition. *Proceedings of the IEEE*, 86(11):2278–2324, 1998.
- [70] Alex Krizhevsky, Geoffrey Hinton, et al. Learning multiple layers of features from tiny images. 2009.
- [71] Vladimir Vapnik. *The nature of statistical learning theory*. Springer science & business media, 1999.
- [72] Martin Arjovsky, Léon Bottou, Ishaan Gulrajani, and David Lopez-Paz. Invariant risk minimization. *arXiv preprint arXiv:1907.02893*, 2019.
- [73] Radoslav Ivanov, James Weimer, Rajeev Alur, George J Pappas, and Insup Lee. Verisig: verifying safety properties of hybrid systems with neural network controllers. In *Proceedings of the 22nd ACM International Conference on Hybrid Systems: Computation and Control*, pages 169–178, 2019.
- [74] Jeremy Cohen, Elan Rosenfeld, and Zico Kolter. Certified adversarial robustness via randomized smoothing. In *International Conference on Machine Learning*, pages 1310–1320. PMLR, 2019.
- [75] Kaiming He, Xiangyu Zhang, Shaoqing Ren, and Jian Sun. Deep residual learning for image recognition. In *Proceedings of the IEEE conference on computer vision and pattern recognition*, pages 770–778, 2016.
- [76] Forrest Iandola, Matt Moskewicz, Sergey Karayev, Ross Girshick, Trevor Darrell, and Kurt Keutzer. Densenet: Implementing efficient convnet descriptor pyramids. *arXiv preprint arXiv:1404.1869*, 2014.

## A Choices of slopes (Cont.)

We present the general recipe of choosing  $\beta$  and  $\gamma$  in the case when the violation point is above the sigmoid function.

	Case 6	Case 7	Case 8	Case 9	Case 10
	$l < \eta, u > \eta$ $\rho''(p) > 0$	$l < \eta, u > \eta$ $\rho''(p) = 0$	$l < \eta, u > \eta$ $\rho''(p) < 0$	$l > \eta \vee u < \eta$ $\rho''(p) \leq 0$	$l > \eta \vee u < \eta$ $\rho''(p) > 0$
$\beta$	$\frac{\rho(p) - \rho(l)}{p - l}$	$\frac{\rho(p) - \rho(l)}{p - l}$	$\min(\rho'(l), \rho'(u))$	$\rho'(p)$	$\frac{\rho(p) - \rho(l)}{p - l}$
$\gamma$	$\frac{\rho(u) - k \cdot u - \rho(p)}{\eta - p}$ where $k = \min(\rho'(l), \rho'(u))$	$\rho'(p)$	$\rho'(p)$	$\rho'(p)$	$\frac{\rho(p) - \rho(u)}{p - u}$

**Table 3:** Choice of the slopes of the piece-wise linear abstraction refinement.

## B Proofs

*Proof.* **Theorem 4.2.** Alg. 1 returns true only if the property holds on a sound abstraction of  $M$ , which following Def. 4.1 means the property holds on  $M$ .  $\square$

*Proof.* **Lemma 4.3.** This can be proved by construction using the  $\beta$  and  $\gamma$  values in Table 1 and Table 3. We next prove that those choices are sound in Lemma 4.4.  $\square$

Before proving Lemma 4.4, we first state the following definitions and facts.<sup>4</sup>

**Definition B.1** (Tangent line). *The tangent line at  $a$  to the function  $f$ , denoted with  $\text{TanLine}_{f,a}(x)$ , is defined as:  $\text{TanLine}_{f,a}(x) = f(a) + f'(a) * (x - a)$ .*

**Definition B.2** (Secant line). *Definition 2.2. Given  $a, b \in \mathbb{R}$ , the secant line at  $[a, b]$  to a function  $f$ , denoted with  $\text{SecLine}_{f,a,b}(x)$ , is defined as:  $\text{SecLine}_{f,a,b}(x) = \frac{f(a) - f(b)}{a - b} * (x - a) + f(a)$ .*

**Proposition B.3.** *Let  $f$  be a twice differentiable univariate function. If  $f''(x) \geq 0$  for all  $x \in [l, u]$ , then for all  $a, x \in [l, u]$ ,  $\text{TanLine}_{f,a}(x) \leq f(x)$ , and for all  $a, b, x \in [l, u]$ , where  $a < b$  and  $a \leq x \leq b$ ,  $\text{SecLine}_{f,a,b}(x) \geq f(x)$ .*

**Proposition B.4.** *Let  $f$  be a twice differentiable univariate function. If  $f''(x) \leq 0$  for all  $x \in [l, u]$ , then for all  $a, x \in [l, u]$ ,  $\text{TanLine}_{f,a}(x) \geq f(x)$ , and for all  $a, b, x \in [l, u]$ , where  $a < b$  and  $a \leq x \leq b$ ,  $\text{SecLine}_{f,a,b}(x) \leq f(x)$ .*

**Proposition B.5.** *Let  $f$  be a differentiable univariate function with non-negative derivative at each point. For all  $\gamma$  if  $\gamma \leq f'(x)$  for all  $x \in [l, u]$ , then  $f(l) + \gamma(x - l) \leq f(x)$  for all  $x \in [l, u]$ .*

*Proof.* **Lemma 4.4.** Cond. 1 and Cond. 2 hold trivially. Since  $q < h(p)$ , for Cond. 3, it suffices to show that  $\forall (m, n) \in \{(x, y) | x \in (l, u) \wedge y = \rho(x)\}$ ,  $n \geq h(m)$ . More concretely, we show that a)  $n \geq \rho(p) + \beta(m - p)$  for  $m \in [l, p]$ , and b)  $n \geq \rho(p) + \gamma(m - p)$  for  $m \in (p, u]$ . We prove this is true for each case in Table. 1.

- **Case 1:** The segment corresponding to  $\beta$  is  $\text{TanLine}_{\rho,p}$ , and Cond. a holds by Prop. B.3. On the other hand, the choice  $\gamma$  is such that  $\gamma \leq \rho'(x)$ , for all  $x \in [p, u]$ . Thus Cond. b holds by Prop. B.5.

<sup>4</sup>These are partially adapted from “Incremental Linearization for Satisfiability and Verification Modulo Nonlinear Arithmetic and Transcendental Functions” by Cimatti et al. We will cite the paper in the revised version of the paper.



- **Case 2:** The segment corresponding to  $\beta$  is  $\text{TanLine}_{\rho,p}$ , and Cond. a holds by Prop. B.3. The segment corresponding to  $\gamma$  is  $\text{SecLine}_{\rho,p,u}$ , and Cond. b holds by Prop. B.4.
- **Case 3:** For Cond. a, we further break it into 2 cases:  $m \leq \eta$  and  $m > \eta$ . In the former case, the line  $\rho(p) + \beta(m-p)$  is below the line  $\rho(l) + \min(\rho'(l), \rho'(u))(x-l)$ , which by Prop. B.5 is below  $\rho$ . When  $m > \eta$ ,  $\rho(p) + \beta(m-p)$  is below the secant line  $\text{SecLine}_{\rho,\eta,p}$ , which by Prop. B.4 is below  $\rho$ . On the other hand, the segment corresponding to  $\gamma$  is  $\text{SecLine}_{\rho,p,u}$ , and Cond. b holds by Prop. B.4.
- **Case 4:** The segments are both secant lines,  $\text{SecLine}_{\rho,l,p}$  and  $\text{SecLine}_{\rho,p,u}$ , thus the conditions hold by Prop. B.4.
- **Case 5:** The segments are both tangent lines,  $\text{TanLine}_{\rho,p}$ , thus the conditions hold by Prop. B.3.

The proof of the soundness of the slope choices in Table. 3 is symmetric.  $\square$

*Proof.* **Theorem 4.5.** We can prove the soundness of  $M''$  by induction on the number of invocations of the ADDPLBOUND method. If it is never invoked, then  $M'' = M'$  which is a sound abstraction. In the inductive case, it follows from Lemma 4.4 that adding an additional piecewise-linear bound does not exclude variable assignments that respect the precise sigmoid function. On the other hand, when  $M[\alpha] \models \Phi$ , the ADDPLBOUND method will be invoked at least once, which precludes  $\alpha$  as a counter-example with respect to  $M''$ . That is,  $M''[\alpha] \models \Phi$ .  $\square$

## C Encoding piece-wise linear refinement using LeakyReLU

We observe that it is possible to encode the piecewise-linear bounds that we add during abstraction refinement using LeakyReLU functions. While we do not leverage this fact, we lay out the reduction to LeakyReLU in this section and leave it as future work to further leverage verification tools supporting LeakyReLUs.

A LeakyReLU  $r_\alpha$  is a piecewise linear function with two linear segments:

$$r_\alpha(x) = \begin{cases} \alpha \cdot x & \text{if } x \leq 0 \\ x & \text{if } x > 0 \end{cases},$$

where  $\alpha \geq 0$  is a hyper-parameter.

Given a piecewise linear function with two linear segments:

$$h(x) - \rho(p) = \begin{cases} \beta(x-p) & \text{if } x \leq p \\ \gamma(x-p) & \text{if } x > p \end{cases}$$

We can rewrite  $h$  as the following:

$$h(x) = \gamma * r_\alpha(x-p) + \rho(p), \text{ where } \alpha := \frac{\beta}{\gamma}$$

Note that the  $\alpha$  value is always valid ( $\geq 0$ ) because both  $\beta$  and  $\gamma$  that we choose are positive. This means that we can potentially encode the piecewise linear bounds as affine and leaky relu layers. For example, the piecewise linear upper bound  $y \leq h(x)$  for a sigmoid  $y = \rho(x)$  can be encoded as

$$a_1 = x - p \tag{6a}$$

$$a_2 = r_\alpha(a_1) \tag{6b}$$

$$a_3 = a_2 + \rho(p) \tag{6c}$$

$$y = a_3 + a_4 \tag{6d}$$

$$a_4 \leq 0 \tag{6e}$$

, where  $a_1, a_2, a_3, a_4$  are fresh auxilliary variables. Eqs. a) and c) can be modeled by feed-forward layers. Eq. b) can be modeled by a leaky relu layer. If we treat  $a_4$  as an input variable to the neural network, Eq. d) can be modeled as a residual connection. This suggest that we could in principle express the abstraction as an actual piecewise-linear neural networks (with bounds on the input variables (e.g.,  $a_4$ ), making it possible to leverage verifiers built on top of Tensorflow/Pytorch.

## D Details on training and CVAEs

### D.1 Dataset

We consider the well-known MNIST and CIFAR-10 dataset. The MNIST dataset contains 70,000 grayscale images of handwritten digits with dimensions  $28 \times 28$ , where we used 60,000 images for training and held 10,000 for testing. The CIFAR-10 dataset contains 60,000 colored images of 10 classes with dimensions  $3 \times 32 \times 32$ , where we used 50,000 images for training and held 10,000 for testing.

To perturb the images, we adapt the perturbations implemented in [10].<sup>5</sup> When training and testing the models, we sample images from the dataset and randomly perturb each image with a strength parameter  $c$  that is sampled uniformly from the ranges given in Table 4.

**Table 4:** Perturbation range in the training data

Dataset	Perturbation	Range of $c$
MNIST	brightness	[.0, .5]
	rotation	[-60, 60]
	gaussian blur	[1.0, 6.0]
	shear	[0.2, 1.0]
	contrast	[0.0, 0.4]
	translate	[1.0, 5.0]
	scale	[0.5, 0.9]
CIFAR10	brightness	[.05, .3]
	contrast	[-.15, .75]
	fog	[.2, 1.5], [1.75, 3]
	gaussian blur	[.4, 1]

### D.2 Architecture

On each dataset, we train a conditional variational encoder (CVAE) with three components: prior network, encoder network, and a decoder network (generator). We also train a set of classifiers. In this section, we detail the architecture of these networks. The architecture of MNIST networks are shown in Tables 5–11. Those of the CIFAR networks are shown in Tables 12–17. The output layers of the generators are activated with sigmoid function. All hidden-layers use ReLU activations.

**Table 5:** Prior

Type	Parameters/Shape
Input	$28 \times 28$
Dense	$784 \times 1$
Dense	$300 \times 1$
Dense	$8 \times 2$

**Table 6:** Encoder

Type	Parameters/Shape
Input	$28 \times 28 \times 2$
Dense	$784 \times 1$
Dense	$300 \times 1$
Dense	$8 \times 2$

**Table 7:** MLP\_GEN<sub>1</sub>

Type	Param./Shape
Input	$28 \times 28 + 8$
Dense	$200 \times 1$
Dense	$784 \times 1$

**Table 8:** MLP\_GEN<sub>2</sub>

Type	Param./Shape
Input	$28 \times 28 + 8$
Dense	$400 \times 1$
Dense	$784 \times 1$

**Table 9:** MLP\_CLASS<sub>1</sub>

Type	Parameters/Shape
Input	$28 \times 28$
Dense	$32 \times 1$
Dense	$32 \times 1$
Dense	$10 \times 1$

**Table 10:** MLP\_CLASS<sub>2</sub>

Type	Parameters/Shape
Input	$28 \times 28$
Dense	$64 \times 1$
Dense	$32 \times 1$
Dense	$10 \times 1$

**Table 11:** MLP\_CLASS<sub>3</sub>

Type	Parameters/Shape
Input	$28 \times 28$
Dense	$128 \times 1$
Dense	$64 \times 1$
Dense	$10 \times 1$

### D.3 Optimization

We implement our models and training in PyTorch. The CVAE implementation is adapted from that in [9]. On both datasets, we trained our CVAE networks for 150 epochs using the ADAM optimizer

<sup>5</sup>[https://github.com/hendrycks/robustness/blob/master/ImageNet-C/create\\_c/make\\_cifar\\_c.py](https://github.com/hendrycks/robustness/blob/master/ImageNet-C/create_c/make_cifar_c.py)

**Table 12:** Prior

Type	Parameters/Shape
Input	$32 \times 32 \times 3$
Dense	$3072 \times 1$
Dense	$300 \times 1$
Dense	$8 \times 2$

**Table 13:** Encoder

Type	Parameters/Shape
Input	$32 \times 32 \times 3 \times 2$
Dense	$3072 \times 1$
Dense	$300 \times 1$
Dense	$8 \times 2$

**Table 14:** CONV\_GEN<sub>1</sub>

Type	Param./Shape
Input	$32 \times 32 \times 3 + 8$
Dense	$32 \times 32 \times 4$
Conv	$3 \times 1 \times 1$ filters, padding 0

**Table 15:** CONV\_GEN<sub>2</sub>

Type	Param./Shape
Input	$32 \times 32 \times 3 + 8$
Dense	$32 \times 32 \times 4$
Conv	$3 \times 3 \times 3$ filters, padding 1

**Table 16:** CONV\_CLASS<sub>1</sub>

Type	Params./Shape
Input	$32 \times 32 \times 3$
Conv	$3 \times 3 \times 3$ filters, stride 3
Conv	$3 \times 2 \times 2$ filters, stride 2
Dense	$25 \times 1$
Dense	$10 \times 1$

**Table 17:** CONV\_CLASS<sub>2</sub>

Type	Params./Shape
Input	$32 \times 32 \times 3$
Conv	$3 \times 3 \times 3$ filters, stride 2
Conv	$3 \times 2 \times 2$ filters, stride 2
Dense	$25 \times 1$
Dense	$10 \times 1$

with a learning rate of  $10^{-4}$  and forgetting factors of 0.9 and 0.999. In addition, we applied cosine annealing learning rate scheduling. Similar to [3], we increase  $\beta$  linearly from  $\beta = 0$  at epoch 1 to  $\beta = 0.01$  at epoch 40, before keeping  $\beta = 0.01$  for the remaining epochs. We use a batch size of 256.

The ERM classifiers on the MNIST dataset are trained with the ADAM optimizer with a learning rate of  $10^{-3}$  for 20 epochs. The classifiers for the CIFAR-10 dataset are trained with the ADAM optimizer with learning rate  $10^{-3}$  for 200 epochs. The classifiers in Sec. 5.3 are trained also all trained with the ADAM optimizer with a learning rate of  $10^{-3}$  for 20 epochs. For PGD, we use a step size of  $\alpha = 0.1$ , a perturbation budget of  $\epsilon = 0.3$ , and we use 7 steps of projected gradient ascent. For IRM, we use a small held-out validation set to select  $\lambda \in \{0.1, 1, 10, 100, 1000\}$ . For MDA, a step size of  $\alpha = 0.1$ , a perturbation budget of  $\epsilon = 1.0$ , and we use 10 steps of projected gradient ascent.

#### D.4 Computing resources

The classifiers used in Subsec. 5.3 were trained using a single NVIDIA RTX 5000 GPU. The other networks were trained using 8 AMD Ryzen 7 2700 Eight-Core Processors.

## E Additional Evaluation of CEGAR

### E.1 Comparison with PRIMA [64]

A recent abstraction-based technique that handles transcendental activation functions is proposed in the PRIMA framework [64], which goes beyond single neuron abstractions and consider convex relaxations over groups of activation functions. In this section, we compare against PRIMA on the *same* sigmoid benchmarks used in its evaluation [64]. We run the PRIMA implementation in the artifact associated with the paper,<sup>6</sup> and run a configuration PRIMA+BaB+CEGAR which is the same as DP+BaB+CEGAR, the configuration we used in Sec. 5, except that we first use PRIMA to derive tighter variable bounds. Both PRIMA and our configurations are run on uniform hardware (the same as described in Sec. 5). Each job is given 16 threads and 30 minutes wall-clock time limit. PRIMA terminates without error on all instances. Table 18 shows the number of verified instances and the average runtime on verified instances by the two configurations. Our configuration is able to consistently solve more instances with only moderate increase on average solving time. This suggests that the meta-algorithm that we propose can leverage the tighter bounds derived by existing abstraction-based methods and boost the state-of-the-art in verification accuracy on sigmoid-based networks.

<sup>6</sup><https://dl.acm.org/doi/10.1145/3462308/full/>

**Table 18:** Comparison with PRIMA [64] on the same benchmarks used in [64]

Model	Acc.	$\epsilon$	PRIMA		Ours	
			robust	time(s)	robust	time(s)
6x100	99	0.015	52	106.5	<b>65</b>	119.5
9x100	99	0.015	57	136.0	<b>96</b>	323.7
6x200	99	0.012	65	197.9	<b>75</b>	260.7
ConvSmall	99	0.014	56	100.5	<b>63</b>	157.8

## E.2 Evaluation on VNN-COMP-21 benchmarks

We also evaluate our techniques on the 36 sigmoid benchmarks used in VNN-COMP-2021. We exclude the benchmark where a counter-example can be found using PGD attack, and evaluate on the remaining 35 benchmarks. In particular, we run a sequential portfolio approach where we first attempt to solve the query with  $\alpha$ - $\beta$ -CROWN [18, 34, 44] (competition version), and if the problem is not solved, we run PRIMA+BaB+CEGAR. Table 18 shows the results. As a point of comparison, we also report the numbers of the top three performing tools [18, 31, 44, 51, 64] during VNN-COMP-21 on these benchmarks.<sup>7</sup> While  $\alpha$ - $\beta$ -CROWN is already able to solve 29 of the 35 benchmarks, with the abstraction refinement scheme, we are able to solve 1 additional benchmark. We note that during the competition  $\alpha$ - $\beta$ -crown did not use up the 5 minute per-instance timeout limitation on any of these benchmarks.<sup>8</sup> This suggests that the solver was not able to make further progress once the analysis is inconclusive on the one-shot abstraction of the sigmoid activations. On the other hand, our technique provides a viable way to make continuous progress if the verification attempt by the state-of-the-art fails.

**Table 19:** Comparison on the VNN-COMP-21 benchmarks

Model	# Bench.	$\alpha$ - $\beta$ -CROWN		VeriNet		ERAN		Ours	
		robust	time(s)	robust	time(s)	robust	time(s)	robust	time(s)
6x200	35	29	12.9	20	2.5	19	145.5	<b>30</b>	83.2

## E.3 Evaluation of an eager refinement strategy

We also compare the lazy abstraction refinement strategy with an eager approach where piecewise-linear bounds are added for each sigmoid from the beginning instead of added lazily as guided by counter-examples. In particular, we attempt to add one piecewise-linear upper-bound and one piecewise-linear lower-bound with  $K$  linear segments for each sigmoid activations. The segment points are even along the x-axis. We try 2 and 3 for the value of  $K$ . We then evaluate on the same MNIST benchmarks as in Table 2. The results are shown in Table 20. While the two strategies are still able to improve upon the perturbation bounds found by the pure abstract-interpretation-based approach DP, the means of the largest certified  $\delta$  are significantly smaller than those of the CEGAR-based configuration we propose. Interestingly, while  $K=3$  uses a finer-grained over-approximation compared with  $K=2$ , the bounds the former can certify is only larger on one of the six benchmark sets. This suggests that the finer-grained abstraction increases the overhead to the solver and is overall not effective at excluding spurious counter-examples on the set of benchmarks that we consider, which supports the need of a more informed abstraction refinement strategy such as the one we propose.

## F Licenses

The MNIST and CIFAR-10 datasets are under The MIT License (MIT). The Marabou verification tool is under the terms of the modified BSD license (<https://github.com/NeuralNetworkVerification/Marabou/blob/master/COPYING>).

<sup>7</sup><https://arxiv.org/abs/2109.00498>

<sup>8</sup>[https://github.com/stanleybak/vnncomp2021\\_results/blob/main/results\\_csv/a-b-CROWN.csv](https://github.com/stanleybak/vnncomp2021_results/blob/main/results_csv/a-b-CROWN.csv)

Dataset	Gen.	Class.	K=2		K=3		DP+BaB+CEGAR		
			$\delta$	time(s)	$\delta$	time(s)	$\delta$	time(s)	# ref.
MNIST	MLP_GEN <sub>1</sub>	MLP_CLASS <sub>1</sub>	0.137 ± 0.043	88.9	0.137 ± 0.042	109.8	<b>0.157</b> ± 0.057	84.1	1.5 ± 1.1
	MLP_GEN <sub>2</sub>	MLP_CLASS <sub>1</sub>	0.109 ± 0.031	114.5	0.109 ± 0.031	199.0	<b>0.118</b> ± 0.049	114.8	1.0 ± 1.1
	MLP_GEN <sub>1</sub>	MLP_CLASS <sub>2</sub>	0.126 ± 0.045	64.0	0.129 ± 0.044	95.9	<b>0.15</b> ± 0.059	120.6	1.2 ± 1.2
	MLP_GEN <sub>2</sub>	MLP_CLASS <sub>2</sub>	0.108 ± 0.038	159.0	0.106 ± 0.036	133.8	<b>0.121</b> ± 0.049	191.6	0.8 ± 1.1
	MLP_GEN <sub>1</sub>	MLP_CLASS <sub>3</sub>	0.132 ± 0.043	139.5	0.131 ± 0.042	190.0	<b>0.146</b> ± 0.059	186.9	1.0 ± 1.1
	MLP_GEN <sub>2</sub>	MLP_CLASS <sub>3</sub>	0.105 ± 0.033	107.1	0.098 ± 0.035	87.5	<b>0.122</b> ± 0.041	163.3	0.6 ± 1.0

**Table 20:** Evaluation results of the eager approach. We also report again the results of DP+BaB+CEGAR, which is the same as Table 2.